HAL
open science

Non-Rigid Registration meets Surface Reconstruction

Mohammad Rouhani, Edmond Boyer, Angel D. Sappa

To cite this version:

Mohammad Rouhani, Edmond Boyer, Angel D. Sappa. Non-Rigid Registration meets Surface Reconstruction. 3DV 2014 - International Conference on 3D Vision, Dec 2014, Tokyo, Japan. hal-01063513v1

HAL Id: hal-01063513

https://inria.hal.science/hal-01063513v1

Submitted on 15 Sep 2014 (v1), last revised 21 Oct 2014 (v3)

HAL is a multi-disciplinary open access archive for the deposit and dissemination of scientific research documents, whether they are published or not. The documents may come from teaching and research institutions in France or abroad, or from public or private research centers.

L'archive ouverte pluridisciplinaire **HAL**, est destinée au dépôt et à la diffusion de documents scientifiques de niveau recherche, publiés ou non, émanant des établissements d'enseignement et de recherche français ou étrangers, des laboratoires publics ou privés.

Non-Rigid Registration meets Surface Reconstruction

Mohammad Rouhani
INRIA Rhône-Alpes
Grenoble
mohammad.rouhani@inria.fr

Angel D. Sappa
Computer Vision Center
Barcelona
angel.sappa@cvc.uab.es

Edmond Boyer
INRIA Rhône-Alpes
Grenoble
edmond.boyer@inria.fr

Abstract

Non rigid registration is an important task in computer vision with many applications in shape and motion modeling. A fundamental step of the registration is the data association between the source and the target under consideration. Such association proves difficult in practice, due to the discrete nature of the information and its corruption by various types of noise, e.g. outliers and missing data. In this paper we investigate the benefit of the implicit representation multi-level Partition of Unity (MPU) for the registration of 3D point clouds from coarse to fine resolutions. Using this flexible surface representation, the discrete association between the source and the target can be replaced by a continuous distance field induced by this implicit interface. This significantly eases the registration by avoiding direct association between points. Moreover, by combining this distance field with a proper deformation term, the registration energy can be expressed in a linear least square form that is easy and fast to solve. Experimental results are provided for point clouds from multi-view data sets. The qualitative and quantitative comparisons show the outperformance and robustness of our framework in presence of noise and outliers.

1. Introduction

Point set registration is a fundamental issue in shape modeling with several applications in computer vision, robotics or computer graphics. This is particularly true in the recent years, as the expansion of affordable 3D sensors and of efficient point based reconstruction techniques have made point cloud processing a popular research domain. Registering two point clouds consists in finding the best deformation that aligns the two sets. Existing works that solve this problem can be classified with respect to the *deformation model* they consider to transform point sets and also to the *distance* they use to measure the similarity between point sets. In the resulting optimization formulation of the registration problem, the earlier defines a solution space while the latter is used to build an objective function to be minimized. Hence both have a strong influence on the convergence to a meaningful solution. In this paper we particularly focus on the distance term and investigate the benefit of distance fields in the case of non-rigid registration.

Independently of the deformation model, that can exhibit various type of rigidity from (*rigid* to *non-rigid*), the distance measure between two point clouds fundamentally relies on the point association scheme that is devised and over which point distances are evaluated. Most of the existing strategies in that respect are based on discrete point associations. Some use the Euclidean distance and associate closest points in a deterministic way, as in ICP [3], or in a probabilistic way, as in [14]. Others better approximate the real distances between the associated shapes by considering normal and curvature information as in [23]. All these distance estimations are very sensitive to noise and outliers and they are prone to errors with missing parts. Moreover, the minimization of these distance approximations often get trapped in local minima.

In this work we experiment a flexible interface (Fig.1(b)) for non-rigid registration with the objective to alleviate the need for discrete point associations. This interface is an implicit function that can define a distance field around the target point set. Interface representations have been successfully used to rigidly register two point sets, e.g., [24] and we consider here their extension to the non-rigid case. The interface induces a gradient field hence relaxing the constraint for explicit point correspondences (see Fig.1(c)). In addition, the interface representation can be implemented in a coarse-to-fine manner in order to avoid local minima. Figure1$(c)-(d)$ illustrates this principle with first a coarse implicit interface that captures the global shape information and then gradually switches to a finer interface that accounts for more details of the shape. The main features of our approach are the following:

1. A new efficient formulation that solves non-rigid registration problem without requiring any correspondence.

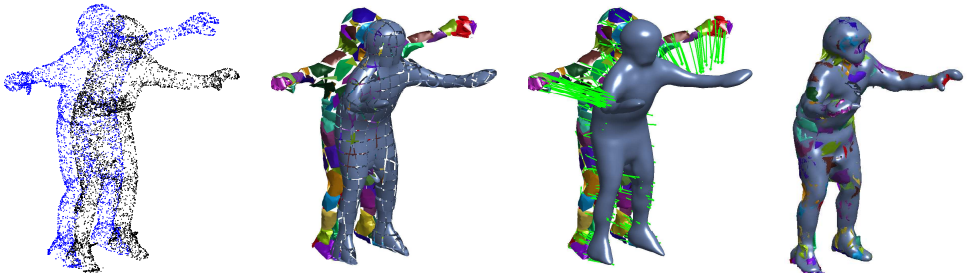

(a) *(b)* *(c)* *(d)*

Figure 1. Using implicit interface for registration: (a) initial pose of the source and target sets; (b) source patches and the local quadrics representing the target; (c) the blended MPU induces a gradient field; (d) deformed source patches fitting the MPU; a coarse-to-fine interface has been used in $(c) - (d)$.

2. The proposed representation allows for coarse to fine strategies.

3. The resulting optimization can be performed by iteratively solving sparse linear system of equations.

4. The approach challenges traditional techniques that consider time consuming discrete point associations are prone to errors with noise, outliers and missing data

The remainder of the paper is as follows. Section 2 discusses related works in surface registration. The approach is detailed in Section 3 . Section 4 presents results and comparisons on public data sets.

2. Related Works

Point set registration consists in finding the best transformation that align two point sets in the same pose and in a single coordinate system. As mentioned earlier, the problem relies on two main aspects, namely the deformation model and the distance measurement. In this section the related works are presented with respect to these aspects.

Deformation model: such model should be defined prior to any rigid or non-rigid registration. Its importance comes from the fact that it defines the parameter space within which the optimization will be performed. It can be simply rigid or affine transformations that are linear with respect to the parameter vector allowing hence for only a few degrees of freedom. When it comes to non-rigid deformation transformations must be more elaborated in order to capture different motions while maintaining surface properties. These transformations can be divided in two main categories: the extrinsic and intrinsic deformations.

In the extrinsic deformation models, the whole space where the object is embedded deforms and the object follows that deformation consequently as a specific part of the space. For instance, In Thin-Plate Spline (TPS) [5], the space is deformed by changing the control weights of some radial basis functions and in FFD [27] a mapping is provided by controlling the B-spline basis functions. Both transformations are widely used to model the deformation especially for medical imaging applications, where some region based information is available. The rigidity of these transformations is controlled by a quadratic regularization term that may penalize many natural motions.

In contrast, the intrinsic deformation models, only consider the manifold itself. Changes are therefore applied directly on the points over the surface instead of the whole space. Laplacian deformation is one the most popular techniques in this category [28] that is widely used in motion capture applications, e.g. [1]. It extracts local geometric properties at each vertex that are assumed to be preserved by transformations. Skinning methods like [17] use embedded skeleton and preserve the distances to the bone during the deformation, while [25] and [12] try to preserve isometric distances between the points.

In our approach, following [6] and [2], the non-rigid deformation is modeled as a combination of locally rigid transformations, which are applied to patches defined on the object shape. However, in order to reach a meaningful result, the compatibility of these local rigid patches must be maintained by some regularization term. For instance, [2] uses a naive stiffness term that imposes the similarity between the neighboring affine matrices. Instead, we consider a very simple rigidity term, proposed in [6], that checks the transformation effects of each patch on its neighbors. This choice hands over a quadratic deformation term that forces the patches to move together, as it is explained in Section 3.

Data association: this is another major aspect to be considered since it defines the distance between the source and target, which has to be minimized during the registration. Iterative Closest Point (ICP) [3] is the most popular technique in that respect, where every source point is paired with its closest corresponding point in the target set and for which the accumulated distance must be minimized in the parameter space. This distance might not be very accurate due to missing points for instance. In [8] and [22] additional local geometric information that includes normals and curvatures are exploited for better distance estimations.

Distance fields are also frequently used in order to precompute the distance (and its derivatives) in a regular grid of voxels [10], [11]. This pre-computation is still based on discrete point associations and the accuracy depends largely on the grid size. Moreover, distance fields may fail in the presence of noise and missing parts. Probabilistic models, like Gaussian Mixture Model (GMM), are also widely used for point associations [14, 15]. In these models every point cloud is seen as a probabilistic distribution and the distance is defined as the correlation of two densities. This can be viewed as a kind of soft-assignment (e.g., RPM [9]) where many points in the target set are considered as the potential (weighted) correspondences of a single source points.

In our approach an implicit interface is used both for representing the target set and speeding up the distance computation. This work extend the rigid registration techniques in [24] and [31] to the non-rigid case by using a powerful implicit representation as the interface [21] in addition to a flexible deformation model as well. Unlike the aforementioned techniques, the proposed method does not require any correspondence search, which reduces the computational cost. It is also robust to noise that is handled twice, during the surface reconstruction and again during the distance estimation. In addition, using the interface allows to perform coarse-to-fine estimations.

Optimization: Computational aspects of the opimization that is performed are also critical for the performance of the registration. Essentially, the optimization allows to move in the deformation parameter space and to search for the best parameters. The complexity of optimization technique changes based on the model. In [10] a distance field has been used to estimate the distance during the rigid registration. The outcome is a distance in a non-linear least squares form that is solved through the Levenberg-Marquadt algorithm. In [26], the optimal TPS parameters are estimated through solving a non-linear system of equations that are obtained by computing some proper integrals over the mesh.

Variational methods are also used to solve the registration problem as an energy minimization problem. In [18] a finite-element method is used to solve a PDE of the warping field. Euler-Lagrange formulation has been used in [31] to reach a smooth gradient field induced by an implicit polynomial. Gradient descent is one of the common techniques to find the optimal deformation in the nonlinear cases [16], [19]. Probabilistic approaches can be seen as an energy minimizing model as well; but, they use a different optimization framework. EM-like algorithm has been used in [20] to align two GMMs.

Linear least squares form, on the other hand, is one the simplest techniques in optimization that results in a closed form solution. In [23] a linear framework for registration is presented by using a curvature based distance estimation, but it still requires a discrete point association. In the current work, we aim at modeling the registration optimization in a least squares form that is the simplest model for optimization. The proposed technique does not need any discrete point association due to the use of implicit interface. Both data term and the deformation energy are chosen in the way that can be easily optimized using a sparse system of linear equations; and at the same time, the local minimums can be avoided using the coarse-to-fine interfaces.

3. Non-rigid Registration using Implicit Interface

In this section the proposed linear framework for correspondence-free *non-rigid* registration is presented. First, the implicit interface and its induced gradient field are introduced and its description flexibility in different resolutions is highlighted. Then, we explain how this interface can benefit the non-rigid registration by providing a new data term. Finally, a sparse system of equation is derived in order to solve our linear least squares function.

3.1. Implicit Interface

Implicit functions are among the most flexible representations for surface reconstruction that do not require any parameterization on the point cloud. These functions describe the objects of interest through their zero sets and provide further information around the objects. The description used in this work is based on the small quadratic patches that are reconstructed over the cells of an oct-tree. The partition of unity technique is applied afterwards in order to provide a global implicit function that is smooth over the space [21]. This interface provides high-level representations from coarse-to-fine, where each of them induces a continuous gradient field that can be exploited for registration (Fig. 2).

Having reconstructed the small quadratic functions $\{f_1, f_2, ...\}$ over the volumetric oct-tree, a smooth global function $\mathcal{F}$ can be reconstructed by blending these patches:

$$\mathcal{F}(\mathbf{x}) = \sum_{i \in \mathcal{N}^{\mathbf{x}}} \hat{w}_i(\mathbf{x}) f_i(\mathbf{x}) \tag{1}$$

where $\mathcal{N}^{\mathbf{x}}$ refers to the set of cells in the neighborhood of $\mathbf{x}$. The weighting functions $\hat{w}_i(\mathbf{x})$ are designed using a radial function of the distance from the center of the cell. These weights must be normalized in order to sum up to one at any point. The global function $\mathcal{F}$ can be viewed as a convex combination of the quadratic patches that are blended smoothly. The influence of neighboring cells can be easily controlled through the blending radius defined in the weights [21]. Figure 2 illustrates how the quadratic patches are blended smoothly in different resolutions. In this work, we are not interested in the visualization power of this reconstruction technique. We, instead, use this tool to obtain

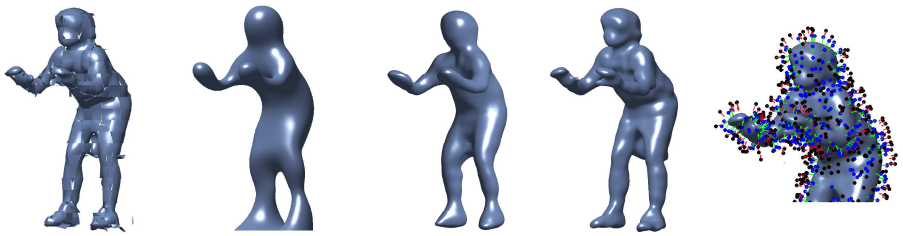

Figure 2. Using MPU to describe a point cloud: $(left)$ small quadratic patches; the rest: the global blending of the local patches in different resolution (coarse-to-fine); $(right)$ the induced gradient field.

a continuous alternative to discrete point association. As illustrated in Fig.2, this function induces a smooth gradient field whose vectors are pointing toward the object in proportion to the distances. Taubin in [29], presents a good distance approximation that can be used in registration [24]:

$$E_{data}(T) = \sum_{\mathbf{x}\in\mathcal{S}} \left(\frac{\mathcal{F}(T(\mathbf{x}))}{\|\nabla\mathcal{F}(T(\mathbf{x}))\|} \right)^2 \tag{2}$$

where T is the optimal deformation to be applied on the source set. Instead of minimizing this non-linear term, [31] considers the integral form of this summation and applies calculus of variation resulting in the following gradient field:

$$\mathbf{g}(\mathbf{x}) = -\gamma \frac{\mathcal{F}(\mathbf{x})}{\|\nabla\mathcal{F}(\mathbf{x})\|^2} \nabla\mathcal{F}(\mathbf{x}). \tag{3}$$

Then, every point is associated with a vector along $\nabla\mathcal{F}$, which is orthogonal to the iso-surface, and its length is proportional to its distance from the zero set. This vector field can be exploited for developing a correspondence-free non-rigid registration method.

3.2. Non-Rigid Registration

Correspondence-free registration based on the implicit interface has been already used in [24] and [31]. In these works only the *rigid* registration problem is considered, while we present a linear formulation for solving the "non-rigid" case using a highly flexible interface. Our formulation also allows a coarse-to-fine approach in order to avoid local minimums. This is accompanied with a flexible patch-based deformation model whose rigidity can be controlled by a quadratic term. As a consequence, a sparse system of linear equations can be derived to solve our correspondence-free non-rigid registration.

A non-rigid deformation can be simply modeled as a combination of local rigid transformations applied on the surface patches [2]. Indeed, the template surface is firstly clustered into small patches using a geodesic distance (Fig.1(b)). Let's $\mathbf{c}_i$ denote the center of the i-th patch. Then, non-rigid deformations can be easily modeled by applying local rigid transformations $T_i(\mathbf{x}) = R_i\mathbf{x} + \mathbf{t}_i$ over these patches. During the registration these rigid parameters can be updated through an affine perturbation that can be captured with 6 parameters denoted as $\boldsymbol{\omega}_i = (\mathbf{u}_i, \mathbf{v}_i)$:

$$\hat{T}_i(\mathbf{x}) = T_i(\mathbf{x}) + K_i\boldsymbol{\omega}_i \tag{4}$$

where $\hat{T}_i$ is the perturbed value of T_i and $\mathbf{K}_i$ is the skew-symmetric matrix of $\boldsymbol{\beta} = R_i(\mathbf{x} - \mathbf{c}_i)$ concatenated with the identity matrix [6].

In the rest of this section we show how to find the affine parameters $\boldsymbol{\omega}_i$ and update the rigid parameters minimizing the data and deformation energy terms.

Data term: Thanks to the linear form of the update vector, the data term can be designed in the least squares form that is favorable for optimization. In the current work the gradient field in (3), induced by the implicit interface, is exploited to update the local rigid transformations. In fact, the source point in the current position $T_i(\mathbf{x})$ must move along the gradient vector $\mathbf{g}(T_i(\mathbf{x}))$ by minimizing the following term:

$$E_{data}(s) = \|K_i\boldsymbol{\omega}_i - \mathbf{g}(T_i(\mathbf{x}))\|^2. \tag{5}$$

This quadratic term is equivalent to imposing three linear constraints on every source point: $K_i\boldsymbol{\omega}_i = \mathbf{g}(T_i(\mathbf{x}))$. These constraints are only applied on those source points whose orientation in the current pose is similar enough to the gradient vector $\nabla\mathcal{F}$ at that point. This normal compatibility check avoids incompatible correspondences. Moreover, through the distance estimation $d = |f|/\|\nabla f\|$ at every source point, those points with the distance bigger than $2\sigma_d$ (standard deviation) are discarded as well.

Deformation term: The local rigid transformations can make a meaningful non-rigid deformation as long as the deformation energy can be controlled. Similar to [6] we penalize the incompatibility of any two neighboring rigid transformations as follows:

$$E_{deform}(\mathbf{x}) = \sum_{(\mathcal{P}^i,\mathcal{P}^j)\in\mathcal{N}} \sum_{\mathbf{x}\in\mathcal{P}^i\cup\mathcal{P}^j} E^{ij}(\mathbf{x}) \tag{6}$$

where $\mathcal{N}$ is the set of all possible neighboring patches and each summand is defined for the points on the pair:

$$E^{ij}(\mathbf{x}) = \|\hat{T}_i(\mathbf{x}) - \hat{T}_j(\mathbf{x})\|^2. \tag{7}$$

This term, in fact, measures the similarity of predictions between the rigid transformation of each patch and its neighboring patches. Following the notation in (4), this term can be described in the least squares form:

$$E^{ij}(\mathbf{x}) = \|K_i\boldsymbol{\omega}_i - K_j\boldsymbol{\omega}_j - (T_j(\mathbf{x}) - T_i(\mathbf{x}))\|^2. \quad (8)$$

Sparse system: In each iteration we aim at finding the best $6N_{\mathcal{P}}$ affine parameters concatenated in the affine vector $\boldsymbol{\omega}$. The data and deformation terms are both in the quadratic form of $\boldsymbol{\omega}$; hence, minimizing the total energy $(E_{data} + \lambda E_{deform})$ is equivalent to solving an over-determined system of equations. The matrix of data term, A_1, includes the entries of K_i and and the right-hand value $\mathbf{b}_1$ contains the coordinates of the gradient field $\mathbf{g}(T_i(\mathbf{x}))$. Similarly, another sparse matrix A_2 is constructed to express the deformation constraints for every point in a pair of patches and b_2 includes the difference in predictions. Finally, the following system of linear equations must be solved to find the update vector:

$$\begin{bmatrix} A_1 \\ \hline A_2 \end{bmatrix} \boldsymbol{\omega} = \begin{bmatrix} \mathbf{b}_1 \\ \hline \mathbf{b}_2 \end{bmatrix}. \quad (9)$$

After finding this vector, we apply SVD decomposition on the covariance matrix between the current points $T(\mathcal{S})$ and updated position $\hat{T}(\mathcal{S})$[1]. Then, every affine update $K_i\boldsymbol{\omega}_i$ can be approximated by the proper rigid parameters $(\hat{R}_i, \hat{\mathbf{t}}_\mathbf{i})$ to update the patch parameters:

$$R_i := \hat{R}_i R_i, \qquad \mathbf{t_i} := \hat{R}_i \mathbf{t_i} + \hat{\mathbf{t}}_\mathbf{i}. \quad (10)$$

4. Experimental Results

The proposed framework has been employed for different non-rigid registration and surface tracking problems. The data sets used in this section are either public [30] or obtained through a multi-view camera environment; the point clouds are equipped with normal vectors as well. The interfaces are reconstructed by the partition of unity weighting technique [21] applied on the quadrics acquired by the 3L algorithm [4]. The implicit interfaces are represented through an oct-tree of depth $6 \sim 8$; the data sets are normalized to lie in the unit cube and the offsets are at the distance of $\delta = 0.01$. Figure 3 illustrates the implicit surfaces describing different frames that are used to avoid point correspondence during the surface tracking. It should be highlighted that the interface can be reconstructed very fast (less than 1 second for 3K points).

Figure 4 shows another example of surface tracking for different frames including: $44, 47, 49, 55, 75$. The surface template for frame 44 is firstly constructed through the geodesic distance as explained in Section 3.2. Then, implicit interfaces are constructed for the rest in order to lead the deformation. Each frame contains a cloud of $30K$ points that are sub-sampled to $3K$. Note that this sub-sampling is only applied to save memory for the deformation term; the MPU interface is able to describe the point clouds of high volume. As illustrated in Fig.4$(bottom)$ these patches deform rigidly following the gradient field induced by these interfaces. It should be highlighted that in this example our method is able to register the first frame directly with the last one without tracking the surfaces in between.

The registration results by the proposed framework are compared with four other methods. Table 1 shows the number of iterations and the accumulated error for all these methods. The first column corresponded to the result of DT-FFD [13], where Free-Form Deformation (FFD) is used to model the transformation. In this method, each data set is described by a discrete distance transform that is constructed for a grid of 80^3 voxels. This method is very slow since it has to compute volume integrals over the distance transforms in order to compute the data term. Moreover, due to the low accuracy of distance transform and the gradient descent method for optimization, there is oscillation in the error values.

Iterative Closest Point (ICP) has been used for comparison in Table 1 for two different deformation and distance estimation models. In the second column a tangent based estimation is used for distance measurement together with FFD [23]. This estimation is used to find the best FFD parameters, while in the third column, ICP is used to find the local rigid parameters [6]. Our experiments show that the ICP-based distance estimation are very likely to get trapped in local minimums. Moreover, as shown in Table 1 the locally rigid deformation, used in our framework, improves the results of ICP-FFD. It is due to the use of a flexible intrinsic deformation instead of warping the whole space.

As the final comparison, we use Gaussian Mixture Model that is a probabilistic approach for point set registration [15]. This method avoids explicit point association by applying an EM-like algorithm. In our implementation we use this approach together with TPS warping, which uses the source points as the control point (resulting in 3×3000 parameters). The result obtained by this method is compared with our approach in Table 1. Note that in each iteration of GMM, 8 EM iterations are applied to update the TPS warping. This method is quite robust to noise but it is very slow and it converges linearly.

Table 1. shows how our method outperforms in terms of error and number of iterations. The accomulated errors in the last three rows are easily calculated since the ground truth correspondences are provided by [30]. For the first two rows, we use the distance from every target point to the tangent plane of its closest source point; it can be better estimated by using curvature information though [22]. The main important point about our approach is to be indepen-

[1] $T(\mathcal{S}) = \{T_i(\mathbf{x}), \mathbf{x} \in \mathcal{S}\}; \hat{T}(\mathcal{S}) = \{T_i(\mathbf{x}) + K_i\boldsymbol{\omega}_i, \mathbf{x} \in \mathcal{S}\}$

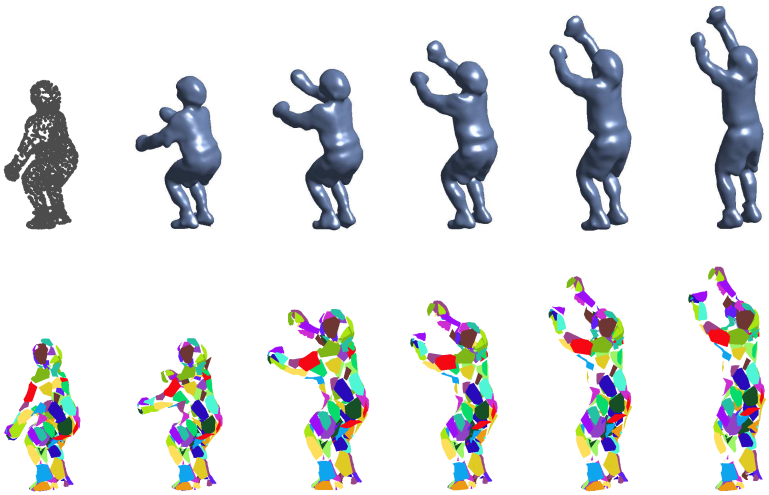

Figure 3. Using MPU interface for surface tracking: (top) the MPU interfaces describing different frames $2, 3, 4, 5, 6$; $(bottom)$ the deformed source patches; notice the patch colors to figure out the correspondences.

Figure 4. 3D point registration using the proposed approach: (top) the MPU interfaces describing different frames $44, 47, 49, 55, 75$; $(bottom)$ the deformed source patches.

dent of point cloud representation. As an example, in Fig.5, the implicit interface can easily tackle noise and missing data such that it interpolate the parts where no data is available. Moreover, the interface can be provided in different resolutions; in Fig.6$(b) - (c)$, for instance, a coarser interface has been used at first, replaced with a finer one after 10 iterations.

A qualitative comparison between different methods is presented in Fig. 5 for a quite challenging pose where the source is orthogonal to the template. Therefore it is very likely that local methods get stuck in some local minimum. The last three examples in this figure use the same deformation model ending with different results though. The EM algorithm has shown a similar result to our approach after 500 iterations while our framework has converged in only 30 iterations. In order to handle our correspondence-free algorithm we initialize a very coarse interface and switched to a coarser one after 15 iterations.

5. Conclusions

In this paper a novel approach for non-rigid registration between two clouds of points has been proposed. The main contribution of this work is to consider the problem in higher level representations, where the source set is clustered into small patches that can deform rigidly, and the target is reconstructed by an implicit interface. Hence, the original problem in the point level is converted into a patches-to-interface problem without requiring any explicit point correspondence. Moreover, the use of implicit interface allows a coarse-to-fine approach that avoids local minimums. The presented method converges in few iterations, in which a sparse system of equations must be solved. The experimental results also illustrates the outperformance in the convergence and the robustness to the noise, outliers and missing parts in the target set.

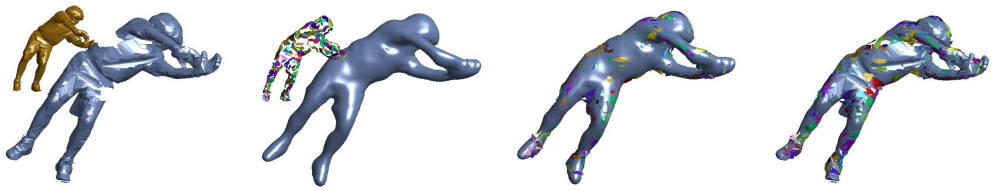

Figure 5. Tackling missing data; (a) the initial pose; (b) MPU interface replaces the target set; (c) the source patches are moved toward the MPU; (d) the converged pose of source patches.

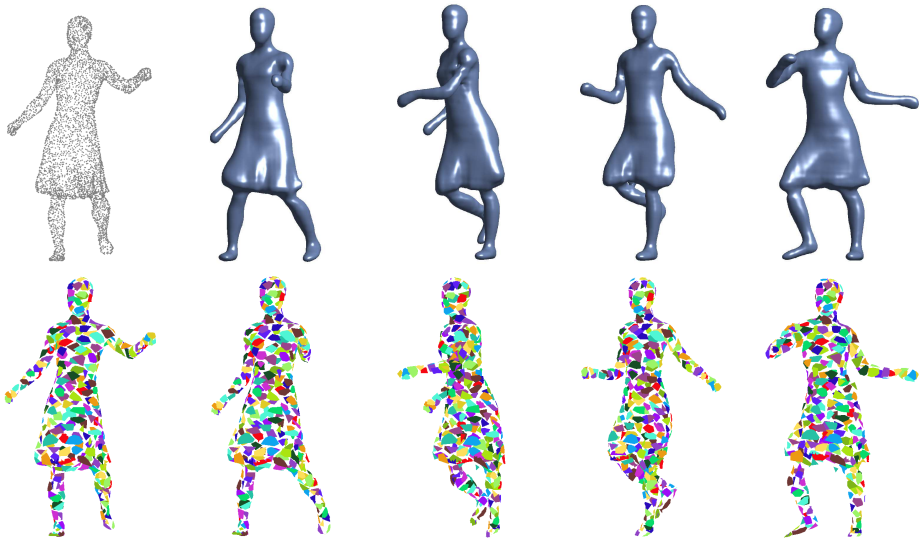

Figure 6. 3D point registration using the proposed approach: (top) the MPU interfaces describing different frames $46, 50, 56, 76, 91$; $(bottom)$ the deformed source patches.

References

[1] E. Aguiar, C. Stoll, C. Theobalt, N. Ahmed, H.-P. Seidel, and S. Thrun. Performance capture from sparse multi-view video. *ACM Transactions on Graphics*, 27(3), 2008. 2

[2] B. Amberg, S. Romdhani, and T. Vetter. Optimal step non-rigid ICP algorithms for surface registration. *IEEE Conference on Computer Vision and Pattern Recognition*, June 2007. 2, 4

[3] P. Besl and N. McKay. A method for registration of 3-d shapes. *IEEE Transactions on Pattern Analysis and Machine Intelligence*, 14(2):239–256, 1992. 1, 2

[4] M. Blane, Z. Lei, H. Çivi, and D. Cooper. The 3l algorithm for fitting implicit polynomial curves and surfaces to data. *IEEE Transactions on Pattern Analysis and Machine Intelligence*, 22(3):298–313, 2000. 5

[5] F. Bookstein. Principal warps: Thin-plate splines and the decomposition of deformations. *IEEE Transactions on Pattern Analysis and Machine Intelligence*, 11(6):567–585, 1989. 2

[6] C. Cagniart, E. Boyer, and S. Ilic. Free-form mesh tracking: A patch-based approach. *IEEE Conference on Computer Vision and Pattern Recognition*, pages 1339–1346, 2010. 2, 4, 5, 8

[7] C. Cagniart, E. Boyer, and S. Ilic. Probabilistic deformable surface tracking from multiple videos. In *ECCV*, pages 326–339, 2010. 8

[8] Y. Chen and G. Medioni. Object modelling by registration of multiple range images. *Image and Vision Computing*, 10(3):145–155, 1992. 2

[9] H. Chui and A. Rangarajan. A new point matching algorithm for non-rigid registration. *Computer Vision and Image Understanding*, 89(2-3):114–141, 2003. 3

[10] A. Fitzgibbon. Robust registration of 2d and 3d point sets. *Image and Vision Computing*, 21(13-14):1145–1153, 2001. 3

[11] K. Fujiwara, K. Nishino, J. Takamatsu, B. Zheng, and K. Ikeuchi. Locally rigid globally non-rigid surface registration. In *International Conference on Computer Vision*, pages 1527–1534, 2011. 3

[12] Q.-X. Huang, B. Adams, M. Wicke, and L. Guibas. Non-rigid registration under isometric deformations. *Computer Graphics Forum*, 27(5):1449–1457, 2008. 2

[13] X. Huang, N. Paragios, and D. Metaxas. Shape registration in implicit spaces using information theory and free form deformations. *IEEE Transactions on Pattern Analysis and Machine Intelligence*, 28(8):1303–1318, 2006. 5, 8

[14] B. Jian and B. Vemuri. A robust algorithm for point set registration using mixture of Gaussians. *International Conference on Computer Vision*, pages 1246–1251, October 2005. 1, 3

[15] B. Jian and B. Vemuri. Robust point set registration using Gaussian mixture models. *IEEE Transactions on Pattern*

Table 1. Comparisons of non-rigid shape registration algorithms: **DT-FFD**: Distance Transform with FFD deformation [13]; **TD-FFD**: Tangent Distance approximation with FFD [23]; **ICP-LR**: Iterative Closest Point with Locally Rigid deformation [6]; **GMM-TPS**: Gaussian Mixture Model with TPS deformation [15] and the proposed approach.

	DT-FFD		TD-FFD		ICP-LR		GMM-TPS		Prop. App.:	
Figure	*Error*	*#Itr*	*Error*	*#Itr*	*Error*	*#Itr*	*Error*	*#Itr*	*Error*	*#Itr*
Fig.4	46.01	*16*	72.26	*30*	49.16	*28*	99.29	*20*	26.40	*24*
Fig.5	46.22	*18*	47.42	*18*	39.76	*18*	57.52	*25*	28.50	*18*
Fig.6$(1-2)$	20.83	*15*	21.99	*27*	9.70	*21*	12.10	*26*	7.34	*14*
Fig.6$(2-3)$	35.76	*22*	38.37	*30*	17.34	*25*	25.10	*39*	13.74	*21*
Fig.7	85.23	*30*	92.89	*30*	130.28	*30*	57.70	*31*	27.71	*30*

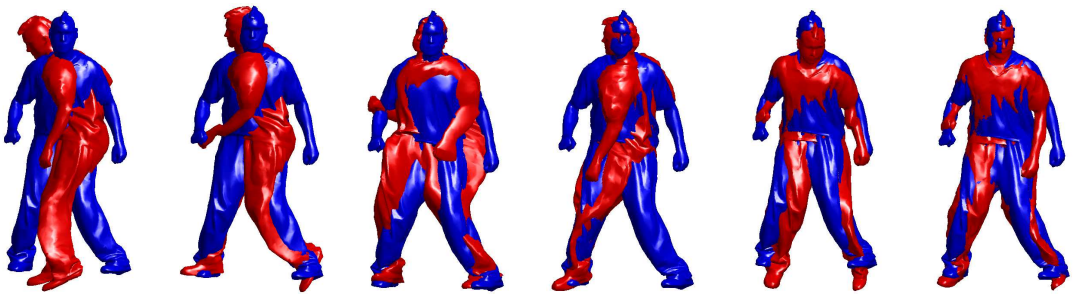

(a) *(b)* *(c)* *(d)* *(e)* *(f)*

Figure 7. Qualitative comparison: (a): initial pose; (b): Linear assignment; (c): Coherent Point Drift [20]; (d): ICP with locally rigid deformation [6]; (e): EM with locally rigid deformation [7]; (f): Our result.

Analysis and Machine Intelligence, 33(8):1633–1645, 2011. 3, 5, 8

[16] T.-Y. Lee and S.-H. Lai. 3d non-rigid registration for mpu implicit surfaces. *IEEE Conference on Computer Vision and Pattern Recognition Workshop*, pages 1–8, 2008. 3

[17] J. Lewis, M. Cordner, and N. Fong. Pose space deformation: a unified approach to shape interpolation and skeleton-driven deformation. pages 165–172, 2000. 2

[18] S. Makram-Ebeid and O. Somphone. Non-rigid image registration using a hierarchical partition of unity finite element method. *International Conference on Computer Vision*, pages 1–8, 2007. 3

[19] H. Munim, A. Farag, and A. Farag. Shape representation and registration in vector implicit spaces: Adopting a closed-form solution in the optimization process. *IEEE Transactions on Pattern Analysis and Machine Intelligence*, 35(3):763–768, 2013. 3

[20] A. Myronenko and X. Song. Point set registration: Coherent point drift. *IEEE Transactions on Pattern Analysis and Machine Intelligence*, 32(12):2262–2275, 2010. 3, 8

[21] Y. Ohtake, A. Belyaev, M. Alexa, G. Turk, and H.-P. Seidel. Multi-level partition of unity implicits. *ACM Transactions on Graphics*, 22(3):463–470, 2003. 3, 5

[22] H. Pottmann, S. Leopoldseder, and M. Hofer. Registration without ICP. *Computer Vision and Image Understanding*, 95(1):54–71, 2004. 2, 5

[23] M. Rouhani and A. Sappa. Non-rigid shape registration: A single linear least squares framework. *European Conference on Computer Vision*, pages 264–277, 2012. 1, 3, 5, 8

[24] M. Rouhani and A. Sappa. The richer representation the better registration. *IEEE Transactions on Image Processing*, pages 5036–5049, 2013. 1, 3, 4

[25] M. Salzmann, J. Pilet, S. Ilic, and P. Fua. Surface deformation models for nonrigid 3d shape recovery. *IEEE Transactions on Pattern Analysis and Machine Intelligence*, 29(8):1481–1487, 2007. 2

[26] Z. Santa and Z. Kato. Correspondence-less non-rigid registration of triangular surface meshes. *IEEE Conference on Computer Vision and Pattern Recognition*, pages 2275–2282, 2013. 3

[27] T. Sederberg and S. Parry. Free-form deformation of solid geometric models. *SIGGRAPH*, pages 151–160, August 1986. 2

[28] O. Sorkine, D. Cohen-Or, Y. Lipman, M. Alexa, C. Rössl, and H.-P. Seidel. Laplacian surface editing. *Symposium on Geometry Processing*, pages 175–184, 2004. 2

[29] G. Taubin. Estimation of planar curves, surfaces, and nonplanar space curves defined by implicit equations with applications to edge and range image segmentation. *IEEE Transactions on Pattern Analysis and Machine Intelligence*, 13(11):1115–1138, 1991. 4

[30] D. Vlasic, I. Baran, W. Matusik, and J. Popovic. Articulated mesh animation from multi-view silhouettes. *ACM Transactions on Graphics*, 27(3), 2008. 5

[31] B. Zheng, R. Ishikawa, J. Takamatsu, T. Oishi, and K. Ikeuchi. A coarse-to-fine IP-driven registration for pose estimation from single ultrasound image. *Computer Vision and Image Understanding*, 117(12):1647–1658, 2013. 3, 4